

Dynamics of dry spots in the liquid film moved by the gas flow in the mini-channel under intensive local heating

Egor Tkachenko^{1,2,*}

¹Kutateladze Institute of Thermophysics, 630090 Novosibirsk, Russia

²Novosibirsk State University, 630090 Novosibirsk, Russia

Abstract. Experimental studies of hydrodynamics and the heat transfer crisis were carried out for a two-phase stratified flow in a mini-channel with intensive heating from a heat source of $1 \times 1 \text{ cm}^2$. It has been established that as the heat flow increases, the total area of dry spots on the heater increases, but when a certain temperature of the heater surface reaches $\approx 100 \text{ }^\circ\text{C}$, the area of dry spots begins to decrease. With the help of high-speed visualization (shooting speed 100000 frames per second), several stages of formation of a dry spot (a typical size of the order of 100 microns) were isolated. It was found that at a heat flux of 450 W/cm^2 about 1 million dry spots per 1 second are formed and washed on the surface of the heater (1 cm^2). The speed of the contact line when dry spot is forming reaches 10 m/s.

1 Introduction

One of the most important problems of thermal physics today is the cooling of microelectronic equipment. At present, the production of processors varies from 14 nm technology to 7 nm technology. New IBM processors use 7-nm transistors. This was made possible by using a silicon-germanium alloy in the construction of a transistor instead of pure silicon, a traditional material for the manufacture of microchips. A normal-sized processor can accommodate more than 20 billion transistors having a size of 7 nm. In addition to reducing the size of the microprocessor unit, the use of a silicon-germanium alloy has improved the switching speed of transistors and reduced energy consumption. The average density of heat flow on the chips of commercially available computers and other electronic devices is up to $200\text{-}300 \text{ W/cm}^2$. In local areas from $100 \text{ }\mu\text{m}$ to several square millimeters, the heat flux density reaches values of 1 kW/cm^2 or even higher (IBM). Next-generation devices can have even higher heat fluxes and impulse loads [1], which requires the output of thermal regulation to a new level.

There are three “classical” methods of heat removal from localized heat sources of high intensity: 1) boiling in microchannels [2], 2) spray cooling [3], and 3) micro-jet cooling. In [4,5], the fourth effective cooling method was proposed, in which the heat removal is

* Corresponding author: egor.tkachenko@mail.ru

caused by the intensive evaporation of a thin liquid film moving in a flat micro- and mini-channel under the action of a gas flow. The method turned out to be an order of magnitude more efficient, in comparison with the falling liquid film [6-8]. In [9-11], studies were carried out that showed the possibility of removing heat fluxes of density up to 1200 W/cm^2 from the heating area $1 \times 1 \text{ cm}^2$ by means of a thin film moving under the action of the gas flow in the channel. In [12, 13] it was shown that such a system can work steadily in a wide range of channel height changes (0.17-2.00 mm) and channel inclination angles to the horizon (0-360°). In [14], heat transfer was studied in a liquid film moving in a channel with an extended heater (at relatively low heat fluxes). In the present work, systematic experimental studies of the flow and rupture of a water film moving in a channel are considered when heated from a local heat source $1 \times 1 \text{ cm}^2$. The dynamics of dry spots is investigated using a high-speed camera with the frequency of up to 100 000 frames per second.

2 Experimental stand

Fig. 1 shows the scheme of the experimental stand. The stand includes a test section, measuring systems, an open gas line and a closed fluid circuit, as well as a system for supply and monitoring of working phases. The stand also includes an automated National Instruments ADC (not shown in Fig. 1).

Working gas – atmospheric air – with a relative humidity of 20-40% and an initial temperature of $25 \text{ }^\circ\text{C}$ is used, which is supplied to the working area by means of an air compressor. The gas flow rate is regulated by the flowmeter and the Bronkhorst flow controller and ranges from 0 to 200 liters/minute.

As working fluid in the experiment, Ultra-pure distilled Milli-Q water is used at an initial temperature of $25 \text{ }^\circ\text{C}$. The liquid is supplied to the working area by means of a gear pump Reglo-Z 183. The flow rate of the liquid is regulated by means of a pump in the range from 4.2 to 420 ml/minute. The design of the test section allows to create flows in the range $Re_1 = 0 - 210$.

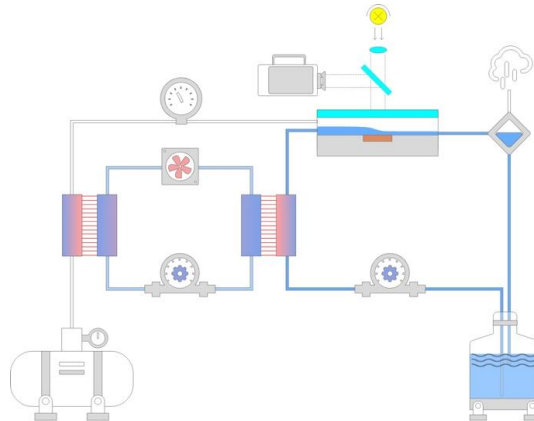


Fig. 1. The scheme of the experimental stand.

Fig. 2 shows the design of the test section – sealed channel with openings for the entry and exit of liquid and gas. The lower part of the channel is a plate made of stainless steel, located on a substrate made of textolite. In the steel plate, a copper cylinder is inserted, acting as a heater. The surface of the copper heater is a square area of $10 \times 10 \text{ mm}^2$. The upper part of the channel is an optical glass, installed to observe the processes in the channel.

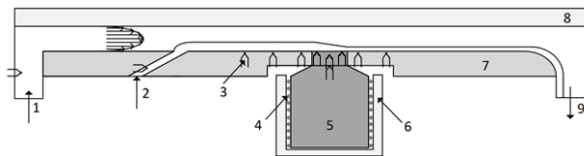


Fig. 2. Design of the test section. 1 – gas nozzle; 2 – liquid nozzle; 3 – thermocouples; 4 – nichrome tape; 5 – copper heater; 6 – thermal insulation; 7 – steel plate; 8 – optical glass; 9 – outlet of liquid and gas.

Thermocouples built into the stainless steel plate and into the copper rod allow to determine the temperature of the working surface. The heat flux is determined by the electrical power released on the heating coil. The thermal conductivity of copper is 400 W/mK, which is more than an order of magnitude higher than the thermal conductivity of stainless steel (15 W/mK). This provides moderate heat flow from the heater to the steel plate. According to estimates, using the measurements of thermocouples embedded in a steel plate, the heat spreading is about 15% at $q > 200 \text{ W/cm}^2$. To reduce heat losses to the atmosphere, the heater was wrapped with a layer of heat-insulating material. According to estimates using thermocouple measurements embedded in the heater, the thermal losses to the atmosphere do not exceed 10% at $q > 400 \text{ W/cm}^2$. Consequently, thermal congestions and losses do not total more than 25% at $q > 400 \text{ W/cm}^2$.

3 Optical visualization

The optical visualization of the experiment was carried out by two methods:

1) Visualization using a Nikon D200 digital camera with a resolution of 3872x2592 pixels (10 Megapixel), with a Micro-Nikkor 105 mm F2.8G VR micro-lens, which allows shooting with a spatial resolution of up to $6 \mu\text{m} / \text{pixel}$. The camera is installed above the surface of the working section perpendicular to the plane of the flow. The survey was conducted at different frequencies, but not less than 3 frames for each stationary mode. Photographs obtained by shooting are one of the main subjects of analysis and comparison.

2) Visualization using high-speed camera FASTCAM SA1.1 CCD. The speed of shooting this camera can vary from 5400 frames per second at a resolution of 1024x1024 pixels and up to 675000 frames per second at resolutions of less than 1024x1024 pixels. The camera is equipped with an optical system of high spatial resolution (up to 500 nm per 1 pixel of the camera sensor).

4 Results

In the visual analysis the following stages of the liquid film rupture were identified with an increase in the heat flux. 1 – formation of a dry spot below the heater. 2 – increase in the dimensions of the first dry spot and the achievement of the surface of the heater. 3 – increase of dry spots on the surface of the heater. 4 – decrease in the area of dry spots on the surface of the heater; 5 – in the pre-crisis moment, the liquid film again covers practically the entire surface of the heater with rapidly appearing and vanishing dry spots on it. And 6 – the moment of crisis, in which the heater is completely dry outed.

An analysis of the experimental photographs was carried out using the ImageJ application. During processing, the places of the heater on which the dry spots formed were assigned a white color and their area in pixels was further considered, knowing the characteristic scale (the length of the heater was 10 mm), the area of the dry spots was translated into mm^2 , then the total area of dry spots, S_{spot} , on the surface of heater was

plotted in relation to the surface area of the heater, S_{heater} , from the heat flux density q . Fig. 3 is a plot of the area of dry spots from the heat flux at various flow rates of liquid and gas.

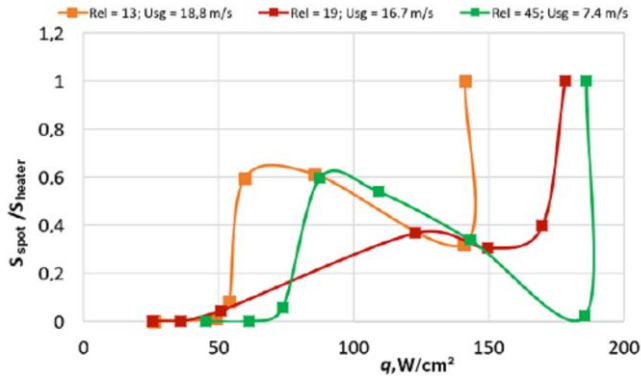


Fig. 3. Dependence of the area of dry spots on the heater surface from the heat flux at various flow rates of liquid and gas.

It can be concluded that the behavior of the liquid film does not qualitatively differ with different heat fluxes. Also there is a qualitative correspondence of the data obtained as a result of processing photos with the help of the ImageJ program and visual observations of the behavior of the liquid film with increasing heat flux density.

With the help of high-speed visualization, the dynamics of formation and washing of a dry spot was obtained. At the initial moment, we can observe a continuous film of liquid, then the film is nonuniform, then it ruptures very quickly, which leads to the formation of a dry spot, further development of this spot, and then after a short period of time, this spot blurs, so the lifetime of one spot is of the order of 1 ms. The size of such spots is about 100 microns. It was also found that with a heat flux of 450 W/cm², about 1 million dry spots per 1 second are formed and washed on the surface of the heater (1 cm²).

For a dry spot the speed of the contact line was calculated (Fig. 4, 5), the maximum speed of the contact line is observed at the time of formation of the dry spot and reaches 10 m/s (because of such high speeds, the frequency of shooting in our experiment does not allow us to understand in detail the mechanism of formation of a dry spot). Further, with an increase in the dimensions of the dry spot, the velocity of the contact line on average takes a value of about 10 cm/s, the speed of the contact line when the dry spot is washed is an order of magnitude greater than increasing, and is of the order of 100 cm/s.

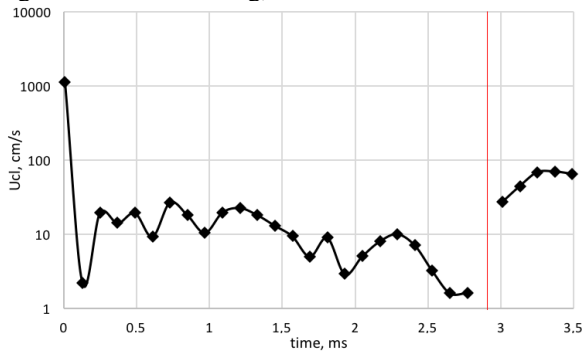


Fig. 4. Speed of the contact line during the formation, increase and washing of the dry spot No 1 (the red line separates the process of increase from the washing of the dry spot).

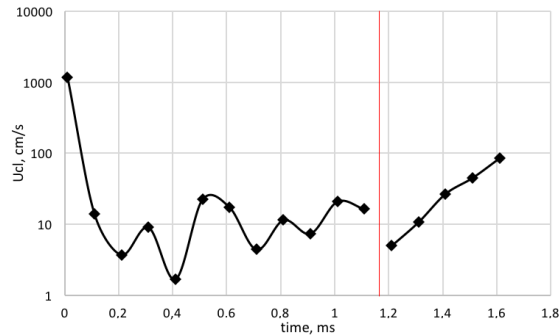


Fig. 5. Speed of the contact line during the formation, increase and washing of the dry spot No 2 (the red line separates the process of increase from the washing of the dry spot).

5 Conclusions

During the experiment, the total area of dry spots increases with increasing heat flow and heater temperature, but when the heater reaches a certain temperature ($\approx 100\text{ }^{\circ}\text{C}$), the total area begins to decrease. The speed of the contact line when forming a dry spot reaches 10 m/s. With an increase in the size of the dry spot, the velocity of the contact line on average takes on the order of 10 cm/s, and when the dry spot is washed, the speed of the contact line is an order of magnitude larger than when increasing, and is of the order of 100 cm/s. It was also found that with a heat flux of 450 W/cm^2 , about 1 million dry spots per 1 second are formed and washed on the surface of the heater (1 cm^2).

The work was supported by the Russian Science Foundation, Project No. 14-19-01755.

References

1. A. Bar-Cohen, C. Holloway, *J. Phys. Conf. Ser.* **745**, 022002 (2016)
2. I. Mudawar, W. Qu, *Int. J. Heat Mass Transf.* **47**, 2045 (2004)
3. J. Kim, *Int. J. Heat Fluid Flow* **28**, 753 (2006)
4. O. A. Kabov, Yu. V. Lyulin, I. V. Marchuk, D. V. Zaitsev, *Int. J. Heat Fluid Flow* **28**, 103 (2007)
5. D. V. Zaitsev, D. A. Rodionov, O. A. Kabov, *Tech. Phys. Lett.* **35**, 680 (2009)
6. O. A. Kabov, D. V. Zaitsev, *Multiphase Science and Technology* **21**, 249 (2009)
7. O. A. Kabov, D. V. Zaitsev, V. V. Cheverda, A. Bar-Cohen, *Exp. Therm. Fluid Sci.* **35**, 825 (2011)
8. E. A. Chinnov, O. A. Kabov, A. V. Muzykantov, D. V. Zaitsev, *Int. J. Heat Technol.* **19**, 31 (2001)
9. E. M. Tkachenko, D. V. Zaitsev, E. V. Orlik, *J. Phys. Conf. Ser.* **754**, 032019 (2016)
10. D. Zaitsev, E. Tkachenko, E. Orlik, O. Kabov, *MATEC Web Conf.* **92**, 01037 (2016)
11. D. Zaitsev, E. Tkachenko, O. Kabov, *EPJ Web Conf.* **159**, 0054 (2017)
12. D. Zaitsev, O. Kabov, *MATEC Web Conf.* **84**, 00043 (2016)
13. E. M. Tkachenko, D. V. Zaitsev, *MATEC Web Conf.* **72**, 01114 (2016)
14. T. Hirokawa, H. Ohta, O. Kabov, *Interfacial Phenomena and Heat Transfer* **3**, 303 (2015)